# LECTURE 16 : MODAL TREATMENT OF ANTENNA SYSTEMS WITH QUASI-OPTICAL FEEDS

## 16.1 INTRODUCTION

Many high-gain antenna systems involve a large main reflector and several subsidiary reflectors and/or lenses. One or more feed-horns provide signal power to, or receive from, the subsidiary optics which together serve as feed to the main reflector. Some large communications ground-stations and radio astronomical telescopes use "beam-wave-guides" (see Figure 16.1) to transport the signal beam from the main reflector to the receiver(s) in such a way that the receivers may remain stationary as the main reflector tracks a source, or in order that, with simple optical switching, different receivers may be used, diplexed or sequentially. Beam-mode analysis can be used to design and to optimise such configurations.

Recent developments of satellite-borne radiometric earth-remote-sensing using millimetre-wave frequencies involve operating in several bands through a single high-performance reflector antenna. One such radiometric system, for example, uses the bands 86-92 GHz, 148-152 GHz, and 175-191 GHz (divided into three sub-bands). In such a system the incoming signals are all received by the same dual-reflector antenna, are separated in a quasi-optical demultiplexer, and delivered to a receiver for each band. Beam-mode analysis is required in the design of a system of this kind.

Some of the uses made of beam-mode analysis in these contexts will be examined in this Lecture.

We begin with the simplest case of a single receive-horn antenna to explain the ideas of *mode coupling*.

## 16.1 Coupling between an incident beam and a receiving feed-horn

In Lecture 5 it was shown how the beam transmitted or radiated by *a source* mounted in a corrugated feed-horn can be analysed into Gaussian beam-modes. I wish now to show how the signal level recorded by *a detector* mounted in a *receiving* feed-horn is determined.

First recall that the beam *transmitted* from any aperture antenna, including feed-horns, can be written as *an angular spectrum of plane-waves* (Lecture 2). This spectrum, $A(k_x,k_y)$, is obtained by Fourier-transforming the field over the aperture. If $A(k_x,k_y)$ is re-written in terms of polar coordinates $\theta,\varphi$ rather than the transverse components of the wave-vector $k_x,k_y$ (using $k_x = k\sin\theta\cos\varphi$ and $k_y = k\sin\theta\sin\varphi$) the result, $A(\theta,\varphi)$, when normalised to unity on-axis, is the *complex antenna pattern* of the aperture antenna; the usual "antenna pattern" is the squared modulus of $A(\theta,\varphi)$. (We are using scalar descriptions of the fields in this discussion, implying treatment of co-polar behaviour only; cross-polar effects could be separately treated along the same lines).

Now, there is a fundamental *reciprocity theorem* in Electromagnetism which relates the transmitting and receiving properties of an antenna. For our purposes it can be conveniently expressed as follows. The relative signal amplitude and phase recorded by a coherent detector in a receiving antenna when a plane-parallel beam is incident upon the antenna from the direction $\theta,\varphi$ are equal to the amplitude and phase of $A^*(\theta,\varphi)$; *relative* here means relative to the amplitude and phase recorded by the detector when an *on-axis* plane-parallel beam, with the same amplitude and the same phase (on a far-field spherical surface) is incident on the antenna.

Now note that an arbitrary incident signal beam can itself be analysed into an angular spectrum of plane waves, $A_S(\theta,\varphi)$ say, or $A_S(k_x,k_y)$ in terms of the transverse components of the wave-vector. The reciprocity theorem then implies that the relative amplitude and phase of the detector output are given by the amplitude and phase of the complex number obtained by evaluating the integral

$$\int_{-\infty}^{+\infty}\int_{-\infty}^{+\infty} A_A^*\,(k_x,k_y)\cdot A_S(k_x,k_y)\,dk_x dk_y \qquad (16.1)$$

where a subscript A (for antenna) has been added to $A(k_x,k_y)$.

Use can now be made of the "generalised Parseval theorem" of Fourier-transform theory, i.e.

$$\int_{-\infty}^{+\infty}\int_{-\infty}^{+\infty} g_1^*\,(k_x,k_y)\cdot g_2(k_x,k_y)\,dk_x dk_y$$

$$\equiv (2\pi)^2 \int_{-\infty}^{+\infty}\int_{-\infty}^{+\infty} f_1^*(x,y)\,.\,f_2(x,y)\,dxdy \qquad (16.2)$$

where $f_1(x,y)$ and $f_2(x,y)$ are arbitrary functions of x,y and $g_1(k_x,k_y)$ and $g_2(k_x,k_y)$ are, respectively, their Fourier transforms. Using this theorem we can re-write Equation 16.1 in terms of the Fourier transforms of $A_A(k_x,k_y)$ and $A_S(k_x,k_y)$, namely the antenna-transmit field $\psi_A(x,y,o)$, and the incident-signal field $\psi_S(x,y,o)$, respectively, in the aperture plane z=0. That is, the relative amplitude and phase of the detector output is given by the complex number which results from an evaluation of the integral

$$\int_C \int \psi_A^*(x,y,z)\cdot\psi_S(x,y,z)\,dxdy \tag{16.3}$$

where the plane of integration, C, is the aperture plane z=0. However, the same result would be obtained if the integral of Equation 16.3 were evaluated over *any* constant-z cross-sectional plane through the beams,

The Case of a Gaussian Antenna Pattern and a Gaussian Signal Beam

Consider the case where both the antenna and the signal beams are *fundamental Gaussian beam-modes*, say $U_A(x,y,z)$ and $U_S(x,y,z)$. The relative amplitude of the coherently detected signal is thus given by the overlap integral, or "inner product", $\langle U_A|U_S\rangle$, i.e.

$$\langle U_A|U_S\rangle = \left|\int_C \int U_A^*(x,y,z)\cdot U_S(x,y,z)\,dxdy\right| \tag{16.4}$$

evaluated over any convenient constant-z plane, C. This integral is straightforwardly evaluated using the explicit form for the fundamental Gaussian beam-mode given in Equation 2.5. If $U_A$ and $U_S$ are both normalised to unity power, i.e. $\langle U_A|U_A\rangle$ and $\langle U_S|U_S\rangle$ are both equal to 1, the maximum possible value of $\langle U_A|U_S\rangle$ is 1 and this value is obtained if the modes $U_A$ and $U_S$ are co-axial and have equal and coincident beam-waists; otherwise $\langle U_A|U_S\rangle$ will be less than 1, indicating, of course, an imperfect match of incident signal to antenna pattern.

Coaxial modes. Consider first modes having a common axis but non-coincident, and not necessarily equal, beam-waists. The following result is obtained when 16.4 is evaluated at a cross-sectional plane, C, in which the beam-width parameters of the two modes are $w_A$ and $w_S$ and the phase-front curvatures are $\kappa_A = 1/R_A$ and $\kappa_S = 1/R_S$.

$$\langle U_A|U_S\rangle = 4\left\{4(w_A/w_S + w_S/w_A)^2 + (kw_Aw_S)^2(\kappa_A-\kappa_S)^2\right\}^{-\frac{1}{2}} \tag{16.5}$$

The expressions in Equation 2.6 for $w(z)$ and $\kappa(z)$ in a fundamental Gaussian beam-mode can be used to re-express this in terms of the beam-waist sizes, $w_{0A}$ and $W_{0S}$, and the *separation of the beam-waists* $\Delta = z_{0A} - z_{0S}$. (The beam-waists are not necessarily real; that for the antenna will usually be virtual - i.e. inside the horn - and so, too, might be the beam-waist for the received signal beam.) The result is

$\bar{\bar{w}} = \sqrt{W_A W_S}$

$$\langle U_A | U_S \rangle = (k\bar{\bar{w}}_0)^2 \left\{(k_2\overline{w_0^2})^2 + (k\Delta)^2\right\}^{-\frac{1}{2}} \qquad (16.6)$$

where $\bar{\bar{w}}_0$ denotes the geometrical mean of $w_{0A}$ and $w_{0S}$, and $\overline{w_0^2}$ denotes the mean of $w_{0A}{}^2$ and $w_{0S}{}^2$. Note that this expression retains nothing to identify the plane C; this confirms the contention made earlier that $\langle U_A | U_S \rangle$ has a value which is independent of the choice of cross-sectional plane over which it is evaluated.

If the beams $U_A$ and $U_S$ have equal beam-waists, $w_{0A} = w_{0S} = w_0$, Equation 16.6 reduces to

$$\langle U_A | U_S \rangle = \left\{1 + (k\Delta/k^2 w_0^2)^2\right\}^{-\frac{1}{2}} \qquad (16.7)$$

The expressions 16.6 and 16.7 show how the efficiency of coupling of the incident signal beam to the receiving antenna varies with the position of the antenna, along the line of incidence of the signal beam, as measured by the separation, $\Delta$, of the respective beam-waists. The larger the value of $kw_0$, the greater the tolerance on $\Delta$.

Note that we have been considering field *amplitude* detection; the *power* coupling is given by the squares of the expressions in Equations 16.3 to 16.7.

<u>Laterally displaced modes</u>. Suppose now that the fundamental modes $U_A$ and $U_S$ have parallel, but not coincident, axes. Evaluation of the overlap integral in Equation 16.4 for a lateral displacement of the axes, d, gives

$$\langle U_A | U_S \rangle = \langle U_A | U_S \rangle_0 \cdot \exp(-d^2/d_e^2) \qquad (16.8)$$

where $d_e^2 = 2\left\{(k^2\overline{w_0^2})^2 + (k\Delta)^2\right\}/k^4\overline{w_0^2}$.

Here $\langle U_A | U_S \rangle_0$ denotes the value for $d \to 0$.

Rotationally displaced modes. If the axes of the modes $U_A$ and $U_S$ are inclined at a (small) angle $\theta$, evaluation of the overlap integral in Equation 16.4 gives

$$<U_A|U_S> = <U_A|U_S>_o \cdot \exp(-\theta^2/\theta_e^2) \tag{16.9}$$

where $\theta_e^2 = \left\{8\overline{w^2}/k^2\bar{\bar{w}}^4\right\} + \left\{\bar{\bar{w}}^4(\kappa_A-\kappa_S)^2/\overline{w^2}\right\}$

where $\kappa_A$ and $\kappa_S$ are the curvatures of the phase-fronts, and $\overline{w^2}$ is the mean-square, and $\bar{\bar{w}}$ the geometric mean, of the beam-width parameters $w_A$ and $w_S$, in the particular cross-sectional plane which contains the point where the mode axes cross. The value of $<U_A|U_S>$ does not depend on the cross-section over which it is evaluated and an expression can be obtained for $\theta_e^2$ which depends only on the beam-*waist* sizes $w_{oA}$ and $w_{oS}$ and on the distances between the beam-waists and the crossing-point of the axis; it is, however, a much more complicated expression than that given above.

## 16.3 Beams which include Higher-order Modes.

To give a good representation of the antenna transmit beam and of the incident signal beam, it may be necessary to include higher-order modes. The coupling coefficient of Equation 16.3 would then involve inner products between modes of different orders. A full derivation of the magnitudes of these coupling coefficients is given by Kogelnik, (see References).

## 16.3 APERTURE EFFICIENCIES OF REFLECTOR ANTENNAS

One use of beam-mode analysis in the context of reflector antennas is the investigation of the dependence of *aperture efficiency* on the design details of the optical system, including, for example, the precise positioning of the receiver's feed-horn. Aperture efficiency is essentially a measure of the degree of coupling between an incoming, on-axis, plane-wave beam and the receiver (assuming no dissipative absorptive losses in the system). 100% aperture efficiency would mean the complete transfer of the power incident over the full area of the antenna's aperture, to the receiver (unattainable, of course).

To determine the aperture efficiency of a Cassegrain antenna (Figure 16.2) for example, we can follow the basic idea traced in the preceding section. The receiver horn is viewed, first, in its transmit mode to find the field it produces at the secondary reflector. The field produced by the incoming plane-wave beam at the secondary, after traversing the main reflector, is then determined (Figure 16.3). The aperture efficiency is then evaluated as a coupling integral. We outline this procedure below (see References).

The incoming plane-wave passes through the primary reflector (which is large so diffraction at its edges will be neglected) to produce after reflection from the secondary reflector, a field of the following form

$$\psi_s(r,z_s,\varphi) = \frac{1}{\sqrt{\pi}a} \cdot \Pi\left[\frac{r}{2a}\right] \cdot e^{\frac{-i\pi r^2}{\lambda z_s}} \qquad (16.10)$$

Here a is the radius of the secondary and $z_s$ the distance from its focus.

$\Pi(x)$ the top-hat function given by

$$\Pi(x) = \begin{cases} 1 \; ; \; |x| \leqslant \frac{1}{2} \\ 0 \; ; \; |x| > \frac{1}{2} \end{cases} \qquad (16.11)$$

The fundamental Gaussian Beam-Mode field generated by a corrugated horn set on the axis of the telescope with a beamwaist offset from the secondary focus by $\Delta$ will be, in the usual notation

$$\psi_\Delta = \left[\frac{2}{\pi w^2}\right]^{\frac{1}{2}} \cdot e^{-\frac{r^2}{w^2}} \cdot e^{-i\left[kz + \frac{\pi r^2}{\lambda R} - \tan^{-1} \hat{z}_\Delta\right]} \qquad (16.12)$$

where the reduced distance is $\hat{z}$ given by

$$\hat{z}_\Delta = \frac{\lambda}{\pi w_o^2} (z-\Delta) \qquad (16.13)$$

The coupling coefficient between these two fields will be

$$C_\Delta = (2\alpha)^{\frac{1}{2}} \left\{\frac{e^{-\alpha+iX}-1}{-\alpha+iX}\right\} e^{\,i(kz-\tan^{-1}\hat{z}_\Delta)} \qquad (16.14)$$

where

taper term

Curvature Difference

$$\alpha = \left[\frac{a}{w_s}\right]^2 ; \quad X = \frac{\pi a^2}{\lambda}\left[\frac{1}{R_s} - \frac{1}{z_s}\right] \qquad (16.15)$$

and $w_s = w(z_s)$, $R_s = R(z_s)$.

From the definition of aperture efficiency . one can see that it is equivalent to the power coupling coefficient

$$C_\Delta C_\Delta^*$$

which leads to $\eta_A$ the aperture efficiency being given by

$$\eta_i \cdot \eta_s \cdot \eta_\Delta \qquad (16.17a)$$

where

$$\eta_i = \frac{2}{\alpha} \; \frac{1 - e^{-\alpha}}{1 + e^{-\alpha}} \qquad (16.17b)$$

underfill feed

is the measure of the taper efficiency,

$$\eta_s = 1 - e^{-2\alpha} \qquad (16.17c)$$

Over-fill

the spillover efficiency and

$$\eta_\Delta = \frac{\cosh\alpha - \cos X}{\left[1+\left[\frac{X}{\alpha}\right]^2\right](\cosh\alpha - 1)} \qquad (16.17d)$$

is the phase efficiency, resulting from axial defocusing of the horn. Fig. 16.4 . shows variations of $\eta_\Delta$ with X for constant $\alpha$. If X is zero, $\eta_\Delta$ is unity, which corresponds to perfect matching of the phase of $\psi_s$ and $\psi_\Delta$. $\eta_i$ and $\eta_s$ are shown in Fig. 16.5 as a function of $\alpha$ and the product has a maximum of 81% when $\alpha$ corresponds to an edge taper of 10.91 dB.

Now extend this analysis by looking at the effect of the higher order modes produced by corrugated-horns. The aperture efficiency is given by

$$\left| \sum_{p=0}^{\infty} A_p \, e^{i\varphi_p} \, C_{\Delta p} \right|^2 \qquad (10.18)$$

where p is the mode number, $A_p$ the normalised amplitude coefficients of the modes generated by the horn and $\varphi_p$ the relative phase slippage between the modes (see Lecture 5; Section 5.2).

One might think that these higher order modes, which contain less than 2.1% of the power transmitted by the horn, would have little effect upon the aperture efficiency. However, there is a clear change in efficiency between the simple fundamental mode model and a model using just the fundamental and the second mode. The effect is quite striking - near the optimum $\alpha$ (edge taper) the efficiency is increased by 7%; using all 11 modes given in Lecture 5 shows less change, 3%. To obtain a precise understanding of the efficiencies of Cassegrain antennas clearly requires consideration of higher-order modes - even with the nearly-pure Gaussian field of a corrugated feed-horn.

More extensive quantitative design information for multi-mirror antennas can be gained by an extension of this kind of beam-mode analysis. Several such studies are listed in the References.

## 16.4 FREQUENCY-INDEPENDENT FEED SYSTEMS

Recent developments of satellite-borne radiometric earth-remote-sensing using millimetre-wave frequencies involve operating in several bands through a single high-performance reflector antenna. One such radiometric system, for example, uses the bands 86-92 GHz, 148-152 GHz, and 175-191 GHz (divided into three sub-bands). In such a system the incoming signals are all received by the same dual-reflector antenna, are separated in a quasi-optical demultiplexer, and delivered to a receiver for each band. Beam-mode analysis is required in the design of a system of this kind. It will usually be required that the antenna pattern be precisely the same in angular-width and beam-efficiency for all frequency-bands. The "frequency-independent" configurations discussed in Lectures 3 and 4 are therefore pertinent.

Figure 16.6 illustrates the idea of a dual-reflector antenna fed by a quasi-optical multiplexing system. Frequency diplexing components are discussed in Lecture 8; we are concerned here with the beam-control optical train in which the multiplexing elements are incorporated.

Figure 16.7 illustrates an approach with a number of desirable attributes; one frequency channel is shown. The feed-horn feeds (in a time-reversed description) a pair of off-axis ellipsoidal reflectors which in turn feed a dual-reflector antenna. If the horn is of a design that produces coincident beam-waists for all its beam-modes (Lecture 5) and is placed so that the beam-waist loction is at the focal distance from the first reflector; and if the two reflectors are separated by the sum of their focal lengths; the field at the beam-waist plane of the horn will be re-created at the focal distance from the second reflector (Lecture 4). And, if that focal distance coincides with the geometrical focal plane of the dual-reflector *combination*, the angular distribution in the antenna pattern will be of the same form as the field distribution in the horn's beam-waist plane, i.e. strongly tapered giving high beam-efficiency.

Note that the relationships between the fields in different planes cited above are independent of frequency (within the range of balanced operation of the horn).

The description above is based on the properties of "ideal lenses" and that leaves two matters for further consideration:

effects of truncation at apertures, and
aberrations and mode-conversion at the off-axis reflectors.

Ways in which design parameters can be chosen to minimise such effects have been given in Lectures 15 and 17. Once a system optical design is arrived at (including, no doubt, folding into small space with plane reflectors) a numerical computational assessment of performance might be made.

## REFERENCES

The following papers deal with beam-mode analyses of the performance efficiencies of reflector antenna systme. The treatment outlined in Section 16.3 and Figures 16.2 to 16.6 are based on the paper by J.W. LAMB.

J.W. Lamb, Quasi-optical Coupling of Gaussian Beam Systems to Large Cassegrain Antennas.
Int.J.Infrared and Millimetre Waves, 7, 1511-1535, 1986.

R. Padman, J.A. Murphy and R.E. Hills, Gaussian Mode Analysis of Cassegrain Antenna Efficiency.
IEEE Trans., AP35, 1093-1103, 1987.

Ta-shing Chu, An Imaging Beam Wave-guide Feed.
IEEE Trans., AP31, 614-619, 1983.

See also

P.S. Kildal and K.R. Jacobsen, Scalar Horn with Shaped Lens Improves Cassegrain Efficiency.
IEEE Trans., AP32, 1094-1100, 1984.

A full derivation of the magnitudes of the coupling coefficients between modes of different orders is given in :

H. Kogelnik, Coupling and Conversion Coefficients for Optical Modes in Quasi-Optics, Microwave Research Institute Symposia Series 14 (Polytechnic Press, New York, 1964).

See also

W.B. Joyce and B.C. DeLoach, Alignment of Gaussian Beams, App.Optics, 23, 4187, 1984.

J.A. MURPHY

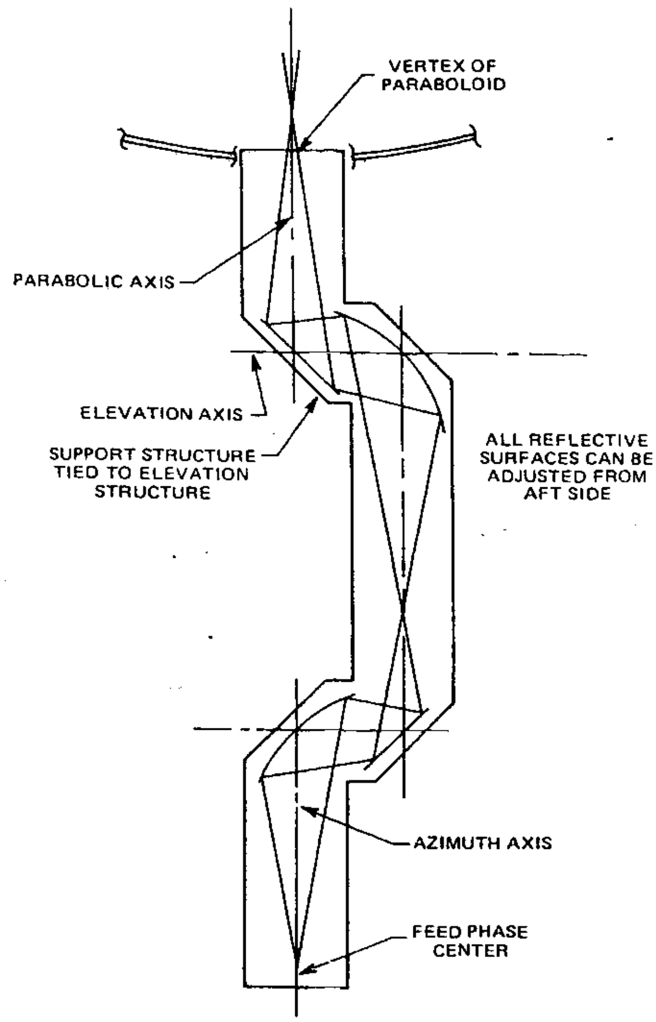


*Beam waveguide optics*

**16.1**

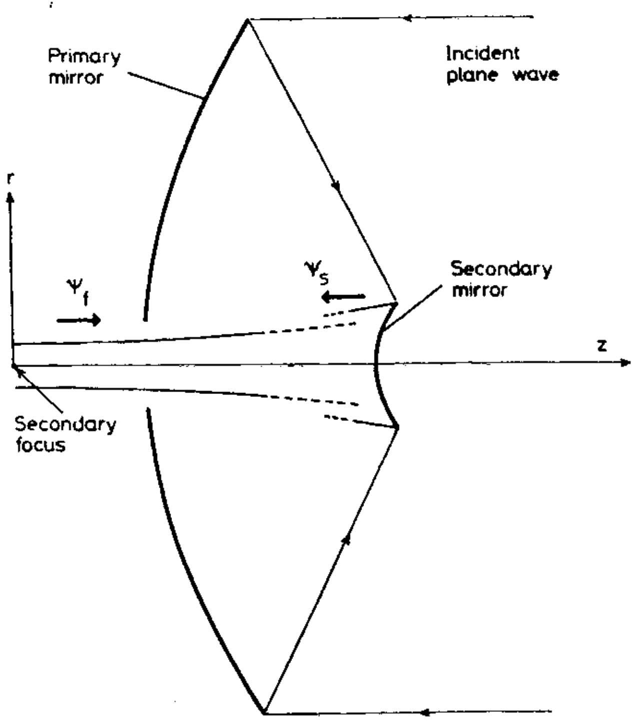


*A plane wave from a distant source incident on the aperture of a Cassegrain antenna is reflected by the primary and secondary mirrors to produce a field $\Psi_s$ propagating toward the feed. In the transmit mode the feed produces a beam $\Psi_f$. The rays diffracted by the edge of the primary are neglected.*

**16.2**

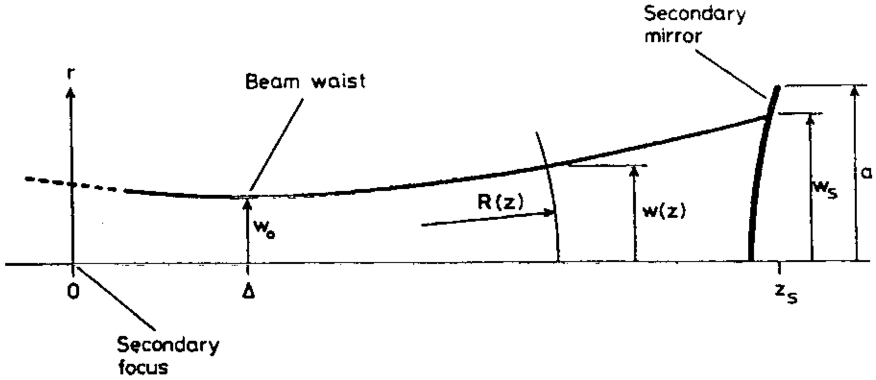


**16.3**

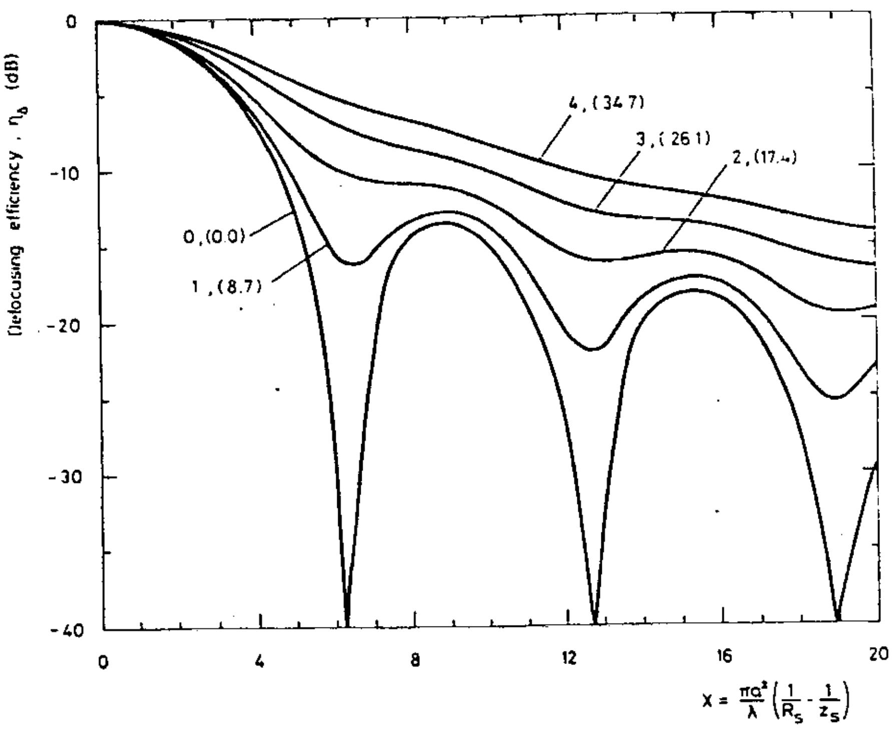


Variation of phase efficiency $\eta_\Delta$ with normalised displacement of beam, X. Curves are labeled by the value of $\alpha$ with the corresponding value of edge taper in dB in brackets.

**16.4**

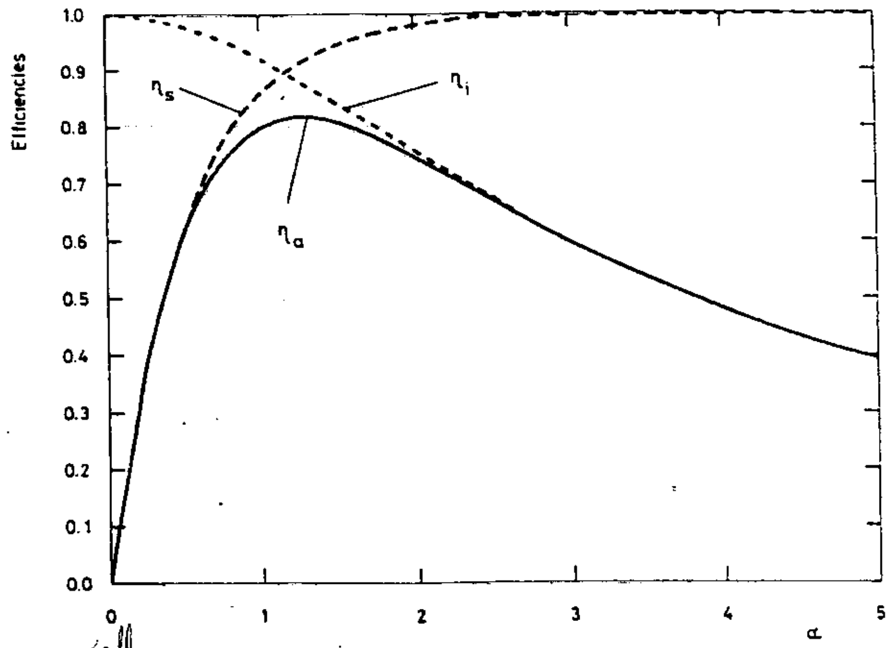


overfill.

*Illumination, spillover and aperture efficiencies (for X=0) as a function of the parameter α.*

$$\alpha = \frac{a}{w_s}$$

**16.5**

$\eta_i$ = Underfill

$\eta_s$ = spill over (overfill

$\eta_a$ =